Electronic Supplementary Information for

A Sequential Template Strategy toward Hierarchical Hetero-Metal Phosphide Hollow Nanoboxes for Electrocatalytic Oxygen Evolution

Yang Wang,[a,b,c,+] Lizhi Sun,[b,+] Longgang Lu,[a] Dongdong Xu,[b] Qingli Hao,[a,*] and Ben Liu[b,c,*]

[a]Key Laboratory for Soft Chemistry and Functional Materials, Nanjing University of Science and Technology, Ministry of Education, Nanjing 210094, China. *E-mail: qinglihao@njust.edu.cn

[b]Jiangsu Key Laboratory of New Power Batteries, Jiangsu Collaborative Innovation Center of Biomedical Functional Materials, School of Chemistry and Materials Science, Nanjing Normal University, Nanjing 210023, China. *E-mail: ben.liu@njnu.edu.cn

[c]College of Chemistry, Sichuan University, Chengdu 610064, China

[+]Yang Wang and Lizhi Sun contribute equally to this work.

1. Electrochemical Tests

All the electrocatalytic measurements were carried out on a CHI 660E electrochemical analyzer. The Linear sweep voltammetry (LSV) was carryed at a scanning rate of 5 mV s^{-1}. The Tafel slopes were calculated using the following formula $\eta=b \log(j/j_0)$, where η is the overpotential, b is the Tafel slope, j is the current density and j_0 is the exchange current density. Chronoamperometry measurements (i-t curves) was carried out under 1.515 V vs.RHE (10 mA cm^{-2}). The electrochemically active surface areas (ECSAs) of the catalysts were evaluated using the double-layer capacitance based on recognized electrochemical method. The CVs were obtained in the non-faradaic region (0.77-0.88 V vs. RHE) at scan rates of 20, 40, 60, 80,100, etc. mV s^{-1}. The potentials were converted to the reversible hydrogen electrode (RHE) by following equation: ERHE = EAg/AgCl + 0.0592*pH + 0.197. The electrochemical impedance spectroscopy (EIS) was carried out in a frequency range from 0.01 Hz to 100 kHz at fixed voltage (1.526 V vs.RHE).

2. Materials Characterization.

SEM was performed using JEOL JSM-7800F. TEM and HRTEM were carried out using a JEOL 2010 transmission electron microscope. HAADFSTEM was taken on an FEI, Talos F200X apparatus, which is equipped with STEM and EDS detectors for elemental mapping analysis. Wide-angle XRD was recorded using a D/max 2500 VL/PC diffractometer (Japan). XPS were performed on a scanning X-ray microprobe (Thermo ESCALAB 250Xi). The N_2 adsorption/desorption isotherms and pore size distribution were analyzed respectively by the BET and BJH method, which were measured on an ASAP 2010 M+C analyzer.

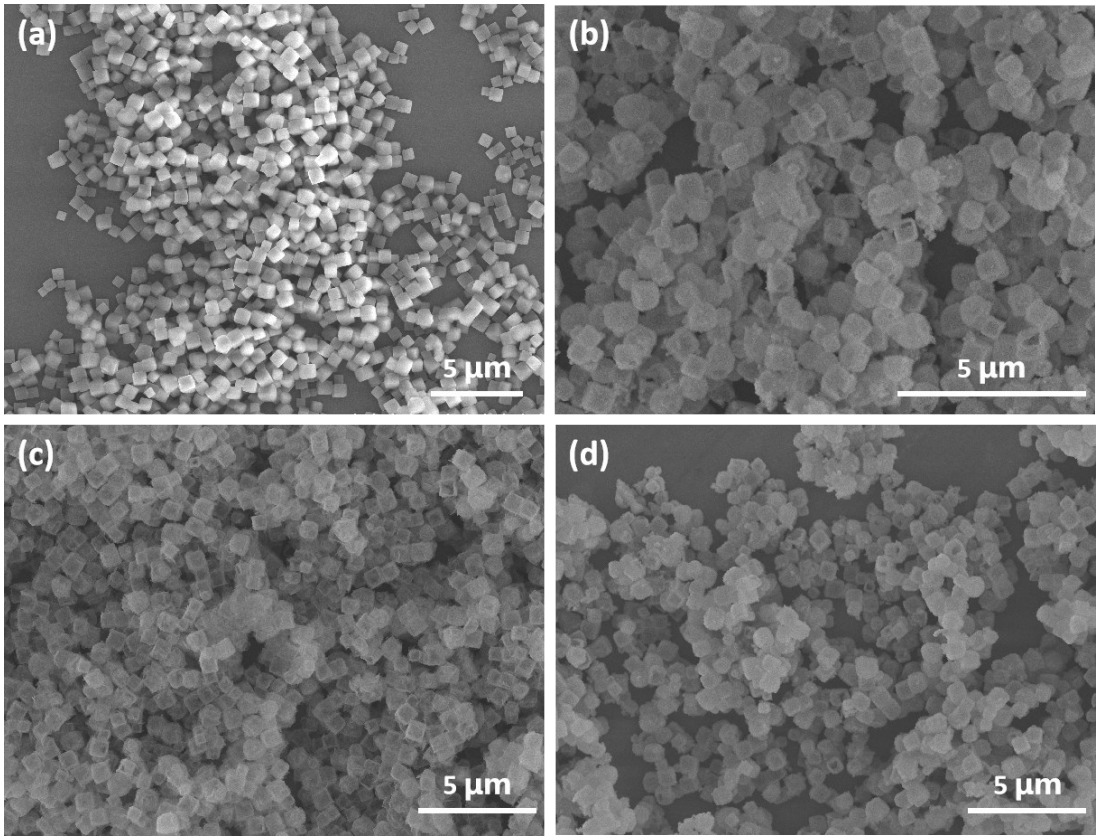

Fig. S1 (a, b, c, d) Low-magnification SEM images of the ZIF-67, Co-Ni LDHs, Co-Co LDHs and Co-Ni LDH@Co-Ni-Fe PBAs.

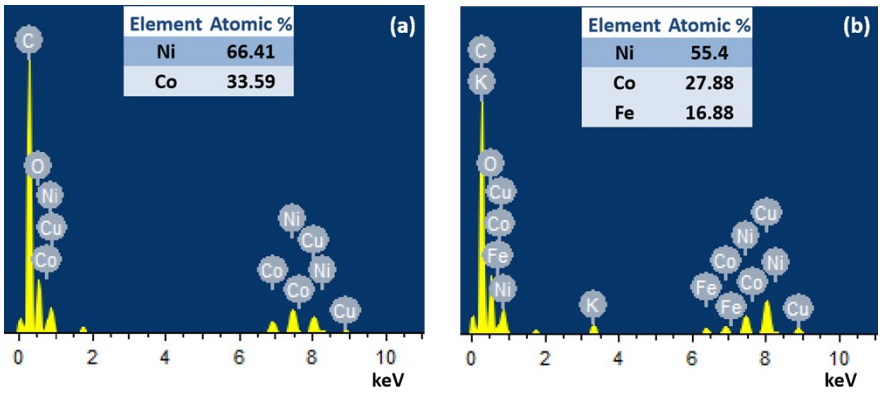

Fig. S2 TEM-EDS elemental analysis of (a) Co-Ni LDHs and (b) Co-Ni LDH@Co-Ni-Fe PBAs.

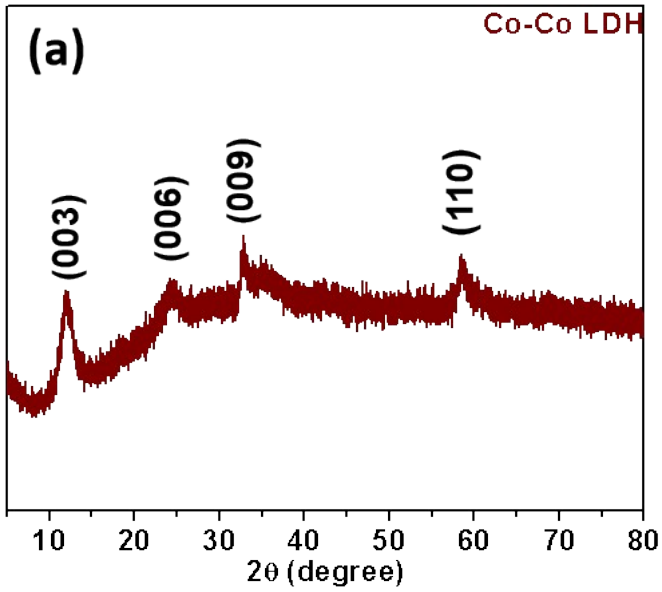

Fig. S3 XRD pattern of the Co-Co LDHs.

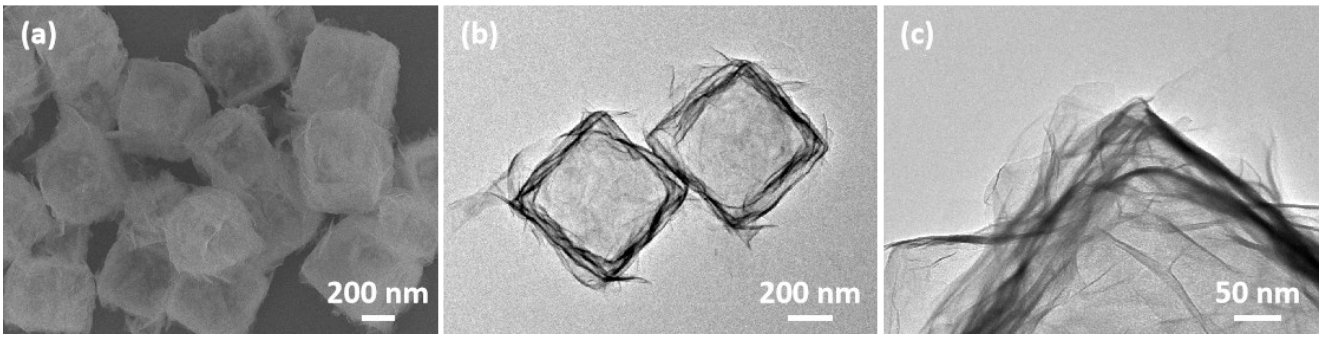

Fig. S4 (a) SEM and (b,c) TEM images of Co-Co LDHs.

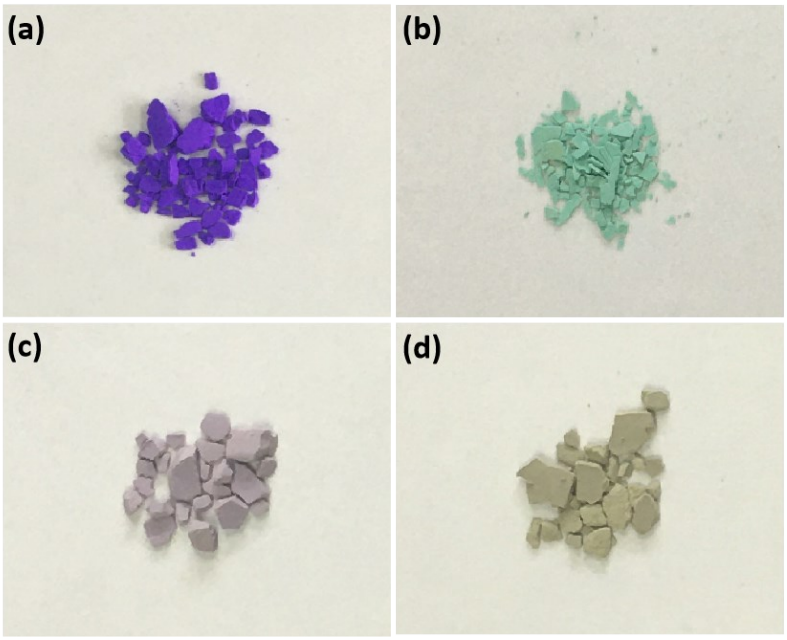

Fig. S5 Photographs of (a) ZIF-67, (b) Co-Ni LDHs, (c) Co-Co LDHs, and (d) Co-Ni LDH@Co-Ni-Fe PBAs costed on papers.

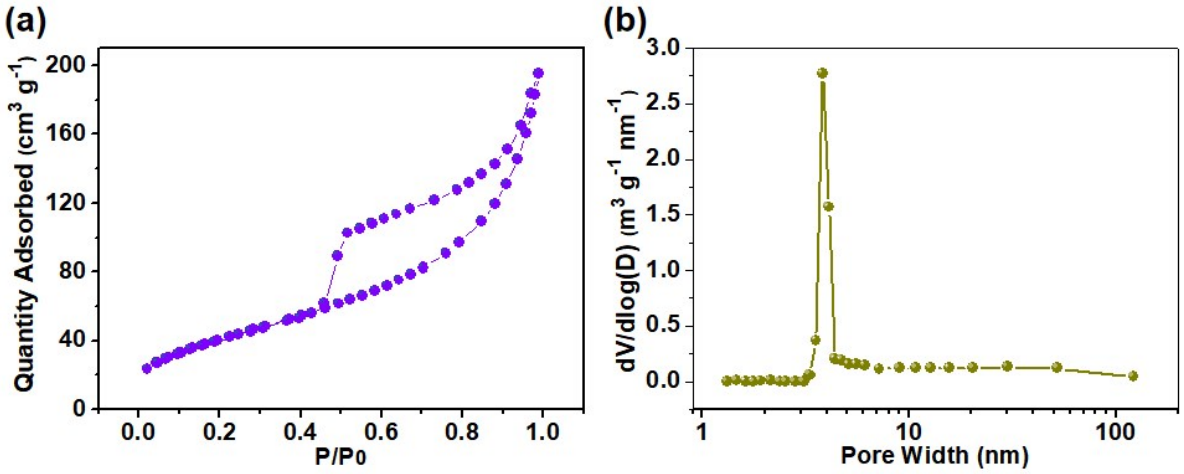

Fig. S6 (a) N_2 sorption isotherms and corresponding (b) pore size distributions of Co-Ni LDH@Co-Ni-Fe PBAs.

Fig. S6a shows the nitrogen adsorption/desorption isotherm plot of Co-Ni LDH@Co-Ni-Fe PBAs, and the Brunauer-Emmett-Teller (BET) specific surface area of Co-Ni LDH@Co-Ni-Fe PBAs is determined to be 151.52 $m^2 g^{-1}$. The corresponding Barrett-Joyner-Halenda (BJH) curve (**Fig. S6b**) indicates the existence of nanosized pores with a narrow pore size distribution centered at 3.4 nm.

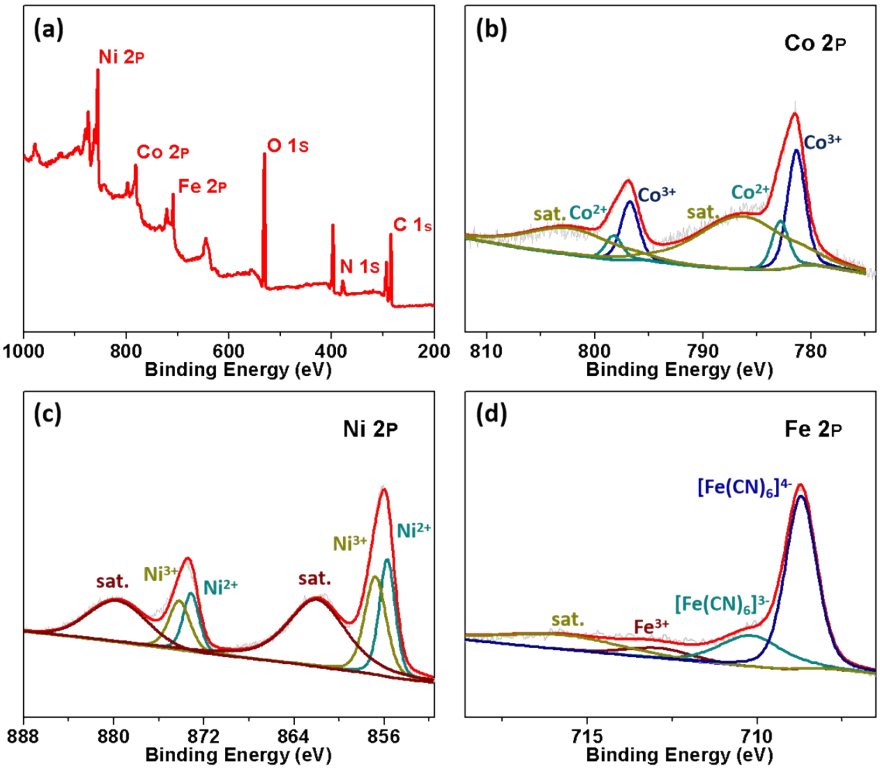

Fig. S7 (a) XPS survey spectrum of Co-Ni LDH@Co-Ni-Fe PBAs; High-resolution XPS spectra of Co-Ni LDH@Co-Ni-Fe PBAs: (b) Co 2p, (c) Ni 2p and (d) Fe 2p regions.

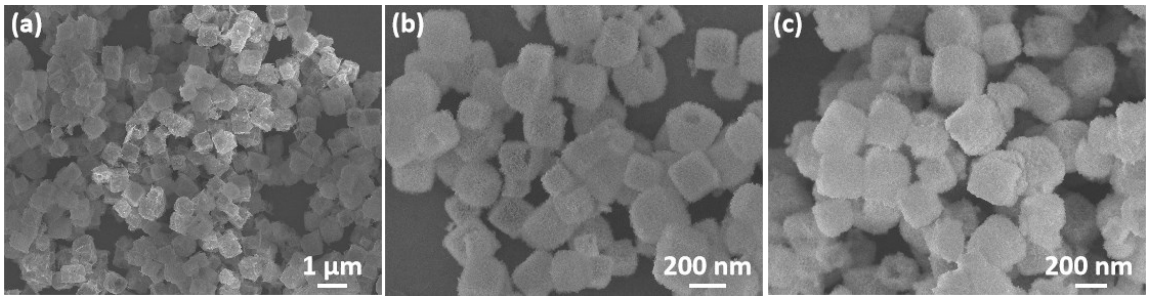

Fig. S8 SEM images of (a) Co-P HNBs, (b) Co-Ni-P HNBs, and (c) Co-Ni-Fe-P HNBs.

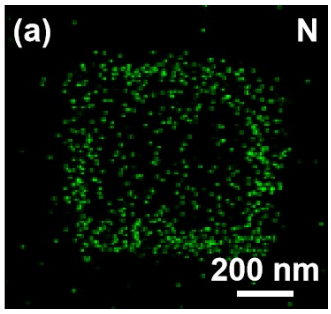

Fig. S9 STEM EDS mapping image of N element in Co-Ni-Fe-P HNBs.

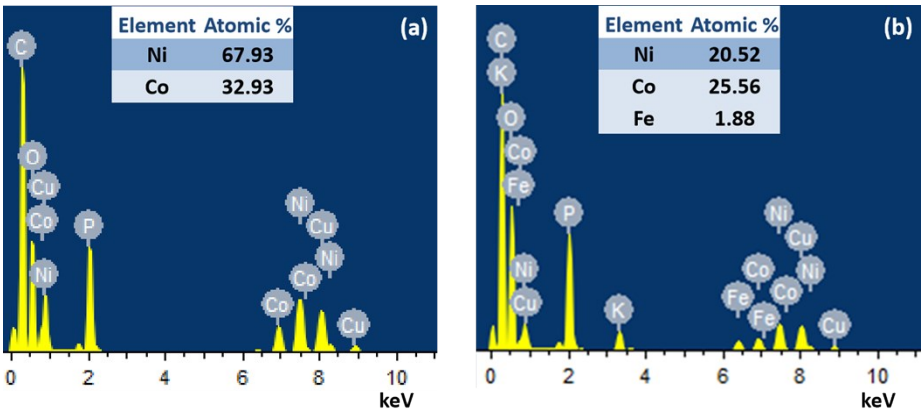

Fig. S10 TEM EDS elemental analysis of (a) Co-Ni-P HNBs and (b) Co-Ni-Fe-P HNBs.

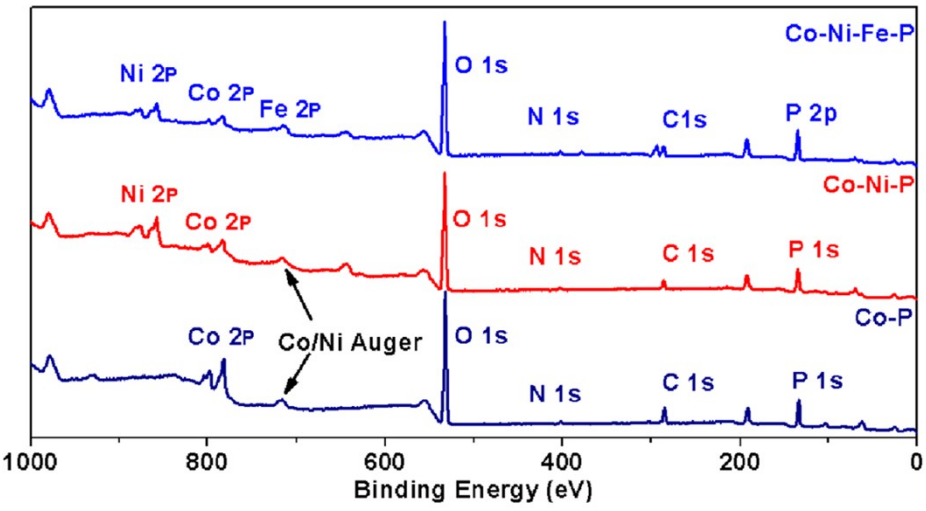

Fig. S11 XPS survey of the Co-P HNBs, Co-Ni-P HNBs, and Co-Ni-Fe-P HNBs.

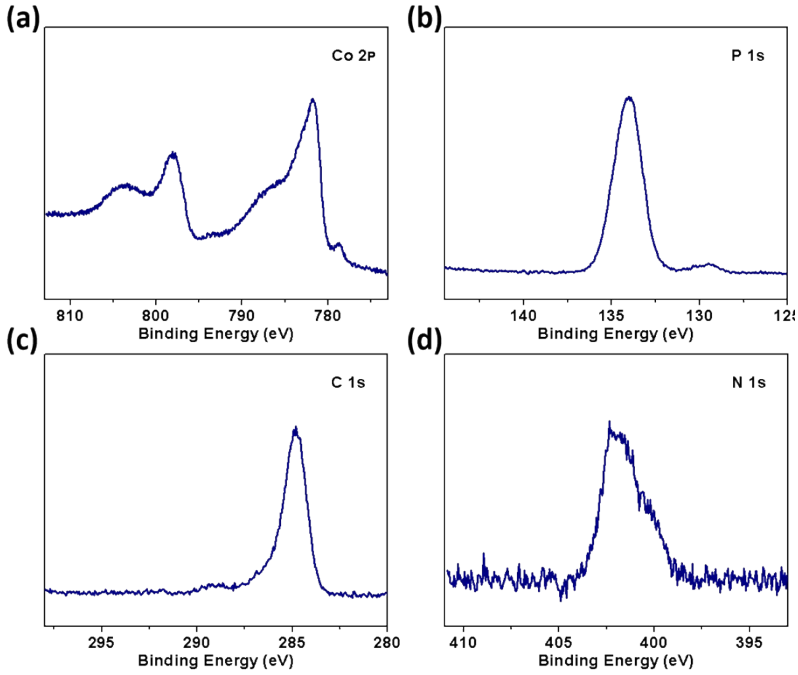

Fig. S12 High-resolution XPS spectra of (a) Co 2p, (b) P 2p, (c) C 1s, and (d) N1s of Co-P HNBs.

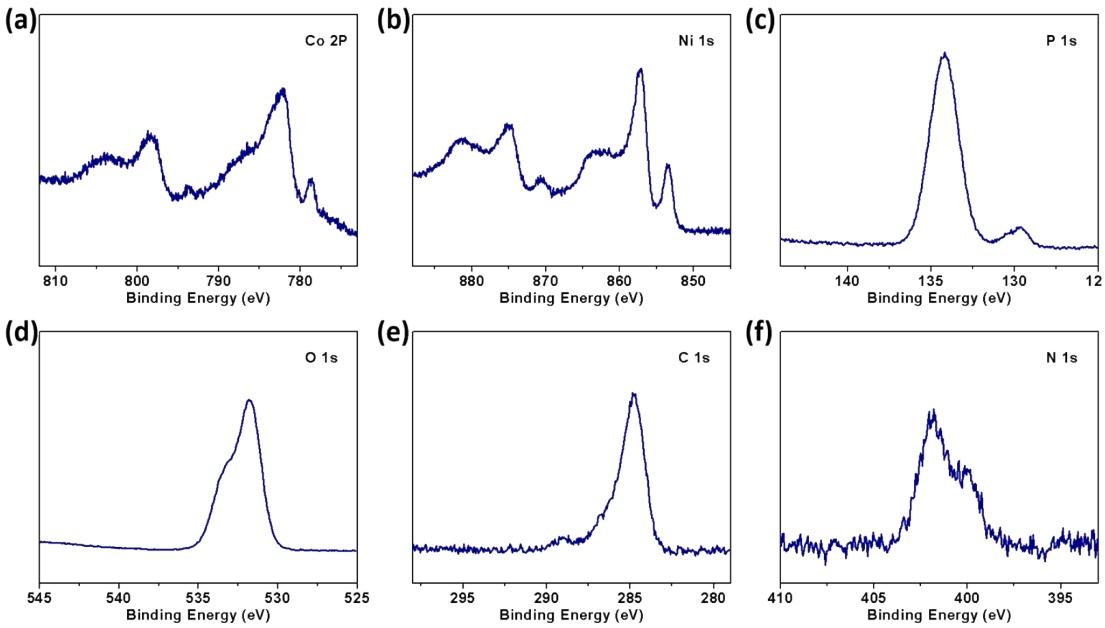

Fig. S13 High-resolution XPS spectra of(a) Co 2p, (b) Ni 2p, (c) P 2p, (d) O 1s, (e) C 1s, and (f) N 1s of Co-Ni-P HNBs.

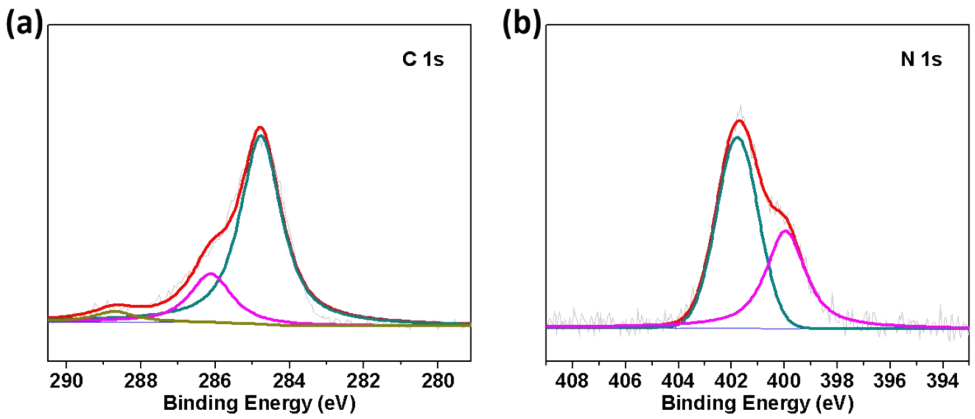

Fig. S14 High-resolution XPS spectra of (a) C 1s and (b) N 1s of Co-Ni-Fe-P HNBs.

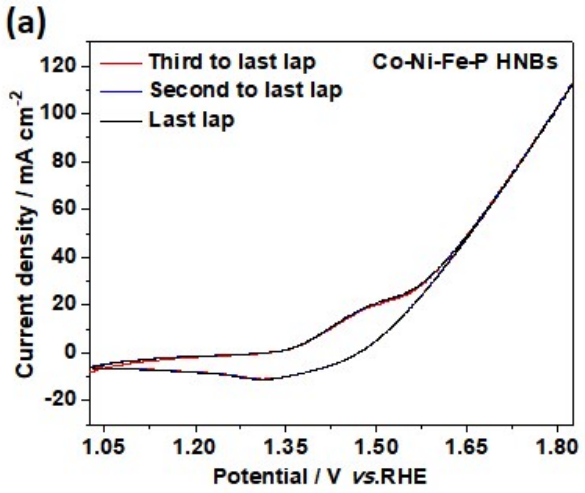

Fig. S15 CV curves of (a) Co-Ni-Fe-P HNBs.

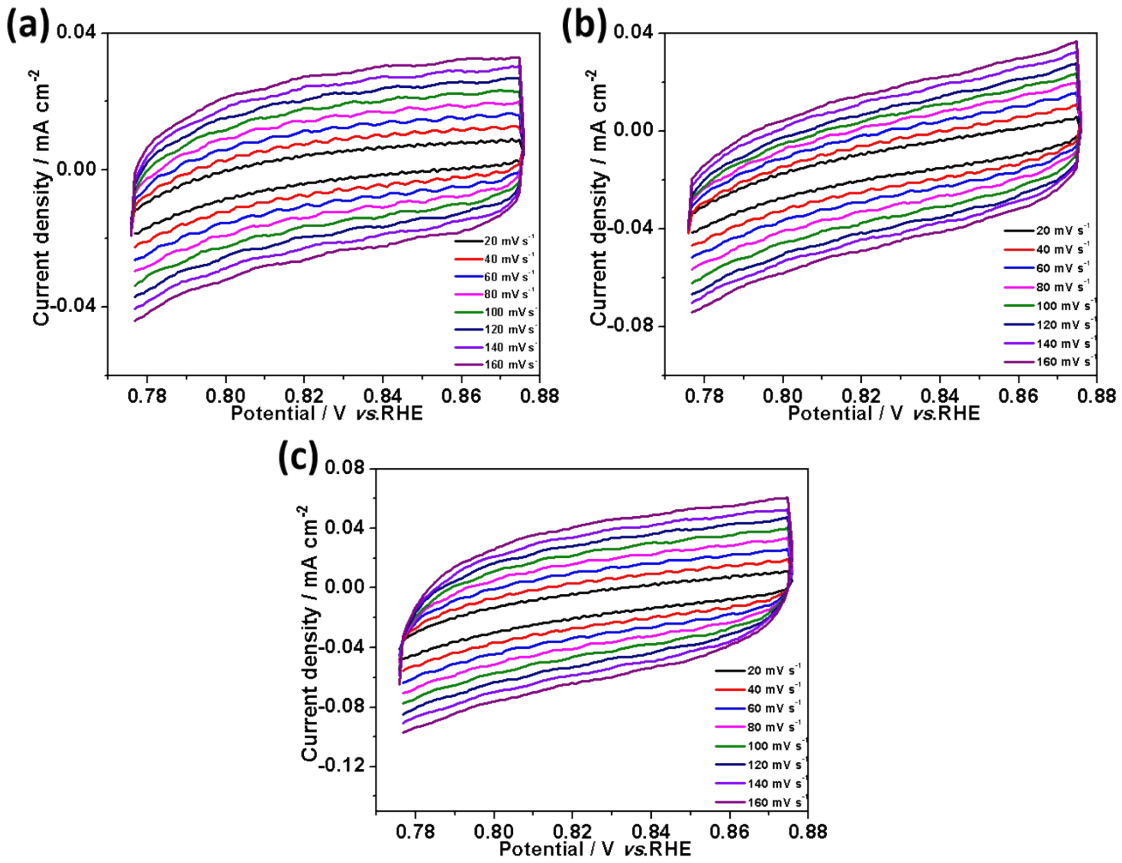

Fig. S16 CV curves of (a) Co-P HNBs, (b) Co-Ni-P HNBs, and (c) Co-Ni-Fe-P HNBs under different scan rates.

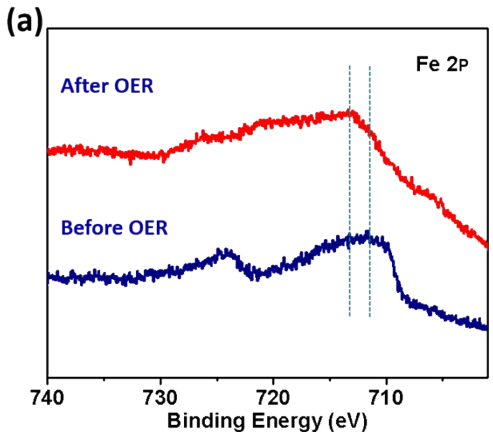

Fig. S17 High-resolution XPS spectra of Fe 2p of Co-Ni-Fe-P HNBs before and after OER tests.

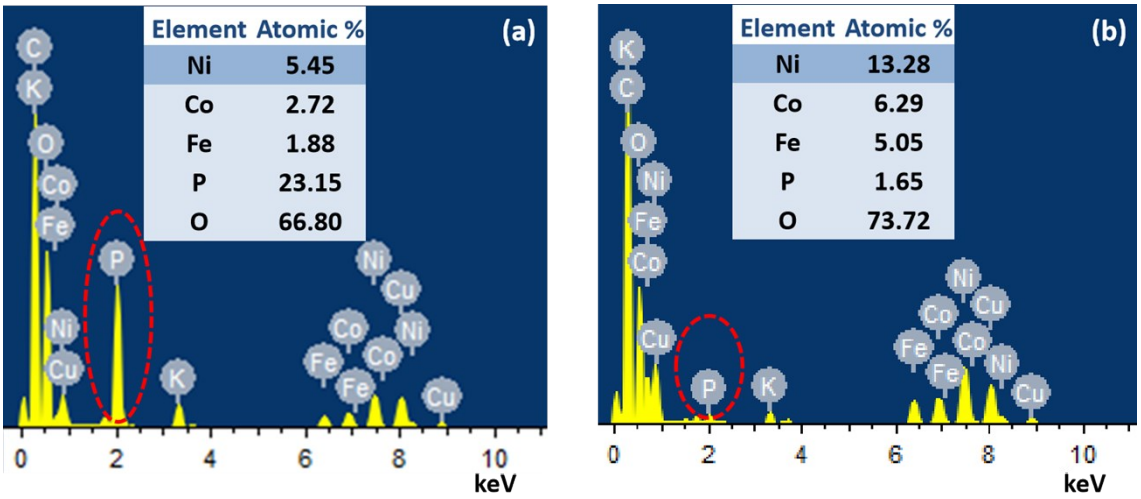

Fig. S18 TEM EDS elemental analysis of Co-Ni-Fe-P HNBs (a) before and (b) after OER tests.

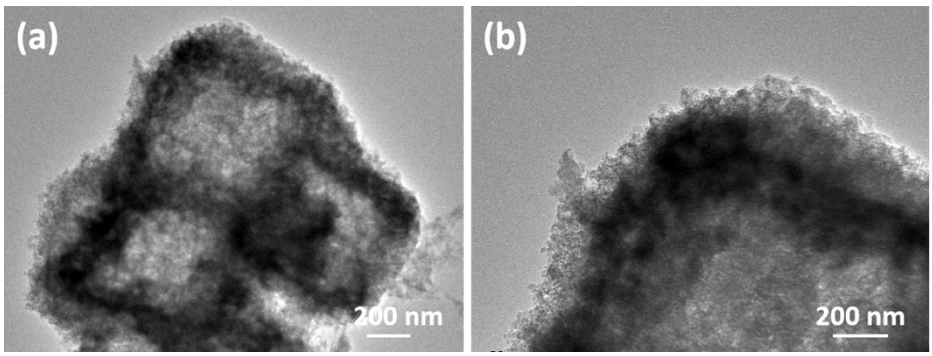

Fig. S19 (a,b) TEM images of Co-Ni-Fe-P HNBs after OER tests.

Table S1 Comparisons of properties of previously reported Fe-Co-Ni-based unitary/hetero-metal catalysts.

Typical examples	Overpotential (mV) at 10 mA cm^{-2}	Ref.
Hierarchical Co-Ni-Fe-P HNBs	249	**This work**
Hierarchical Co-Ni-P HNBs	287	**This work**
Hierarchical Co-P HNBs	324	**This work**
CoP nanoframes	323	*ACS Catal.* **2019**, *10, 412*
CoP@CNs	326	*Adv. Mater.* **2020**, *32, 2003649*
CoP/NCNHP	310	*J. Am. Chem. Soc.* **2018**, *140, 2610*
Ni_2P@C/G	285	*Chem. Commun.* **2017**, *53, 8372*
Ni–P Nanoplates	300	*Energy Environ. Sci.* **2016**, *9, 1246*
Co-Fe-P nanoframes	298	*Chem. Sci.* **2019**, *10, 464*
CoNiP nanosheets	280	*J. Am. Chem. Soc.* **2018**, *140, 5241*
Ni-Co-P hollow nanobricks	270	*Energy Environ. Sci.* **2018**, *11, 872*
Fe–Co–P nanoboxes	269	*Energy Environ. Sci.* **2019**, *12, 3348*
CoP@FeCoP micro-polyhedra	238	*Chem. Eng. J.* **2021**, *403, 126312*
Honeycomb NiCoFeP/C	270	*Chem. Commun.* **2019**, *55, 10896*
NiCoFe hollow nanobox	273	*Small* **2018**, *14, 1802442.*